International Journal of Computer Science and Information Technology
ISSN: 3005-9682 (Print), ISSN: 3005-7140 (Online) | Volume 7, Number 3, Year 2025
DOI: https://doi.org/10.62051/ijcsit.v7n3.11
Journal homepage: https://wepub.org/index.php/IJCSIT/index

Weighted Dynamic Brain Network Feature Analysis in Schizophrenia

Jiatian Li, Guimei Yin *

School of Computer Science and Technology, Taiyuan Normal University, Jinzhong 030619, China

ABSTRACT

Most existing schizophrenia studies employ graph neural network classification based on static brain network structures, neglecting temporal dynamics. Alternatively, they typically introduce dynamic elements solely at the node feature or graph structure level, thereby limiting the models' expressive capabilities. To fully explore the spatio-temporal characteristics of EEG signals, this paper proposes a temporal dynamic graph convolutional network (TDGCN) based on temporal features. It simultaneously introduces temporal dynamic modeling mechanisms at both the node feature and graph structure levels. Wavelet packet-based statistical features and LSTM are used by the model to generate time-varying dynamic weight. Dynamically optimized graph structures and node features are fed into the GCN by the model, and then features are adjusted through a channel gating mechanism after the convolutional layer. Thus, the approach facilitates efficient modeling and classification of the dynamic evolution of brain regions. Experiments on the first-episode schizophrenia resting-state EEG dataset demonstrate that TDGCN achieves optimal performance in the gamma band, achieving an accuracy of 93.85% and outperforming baseline models across multiple evaluation metrics. Ablation experiments validated the crucial role of temporal dynamic weight and dual-layer dynamic graph modeling, demonstrating TDGCN's ability to effectively capture the spatiotemporal non-stationarity of brain networks in schizophrenia patients. This offers novel insights for intelligent auxiliary diagnosis of psychiatric disorders.

KEYWORDS

Schizophrenia; EEG; Temporal features; Dynamic brain network; Graph convolutional networks

1. INTRODUCTION

Schizophrenia is a highly debilitating chronic mental disorder that significantly impairs an individual's cognitive and social functioning [1, 2]. In recent years, electroencephalography (EEG) has been extensively employed in the auxiliary diagnosis of psychiatric disorders owing to its high temporal resolution and non-invasive nature as a method for assessing brain function [3-5]. Given its pronounced temporal non-stationarity and complex spatial distribution, effectively extracting its discriminative spatio-temporal features has become a significant area of current research [6, 7].

Compared to traditional machine learning approaches, graph neural networks (GNNs) within deep learning can more effectively process data with non-Euclidean structures, thereby demonstrating significant advantages when modeling the complex spatial relationships between EEG signal channels [8, 9]. Yin et al. [10] proposed a GCN-based automatic identification model for schizophrenia, achieving an accuracy rate of 90.01% and enabling effective classification of first-episode schizophrenia patients. Ma et al. [11] achieved an accuracy rate of 91.07% across 65 hand gestures in a gesture recognition task using high-density surface electromyography (HD-sEMG). This was accomplished by constructing muscle maps and integrating spatio-temporal convolutions.

However, existing methods predominantly employ fixed graph structures, failing to capture the dynamic characteristics of connection relationships as they evolve over time. This limitation constrains the model's ability to analyze non-stationary signals.

Furthermore, node features often neglect temporal information. EEG signals inherently exhibit high dimensionality, multi-channel characteristics, and strong time-varying properties. Most methods employ only a single feature or simple concatenation, which adversely affects recognition and classification performance. Zhao et al. [12] proposed the Mutual-Cross-Attention (MCA) mechanism, which fuses bidirectional attention with differential entropy (DE) and power spectral density (PSD) features, achieving over 99% accuracy on the DEAP dataset. However, such methods still lack effective utilization of dynamic temporal information.

To address the aforementioned issues, dynamic neural networks (DNNs) [13] have gained increasing attention in recent years by modeling graph structure evolution through attention mechanisms or sequential networks [14, 15]. Guo et al. [16] proposed the dynamic graph convolutional network (DGCN), which utilizes long short-term memory (LSTM) networks to learn the dynamic evolution of the road network's Laplacian matrix, thereby enhancing traffic prediction accuracy. Leng et al. [17] employed a prototype embedding-based dynamic graph network to construct structural brain networks from T1-weighted MRI, achieving state-of-the-art performance in predicting cognitive impairment. However, existing dynamic networks typically only consider unilateral dynamics of nodes or graph structures, lacking a dual-level dynamic mechanism.

To this end, this paper proposes a temporal dynamic graph convolutional network (TDGCN), which introduces dynamic mechanisms at both the node feature construction and graph structure modeling levels. By employing wavelet packet transform (WPT) and LSTM to model node temporal variations, it achieves dual dynamic regulation. Additionally, a channel gating mechanism is incorporated to enhance the network's ability to capture the dynamic evolution characteristics of EEG in schizophrenia.

2. METHODS

The TDGCN schizophrenia classification model proposed in this paper features an overall structure as depicted in Figure 1. It primarily comprises three submodules: (1) temporal dynamic weight (TDW) construction; (2) dual-level dynamic brain network modeling; and (3) a graph convolutional neural network classification framework.

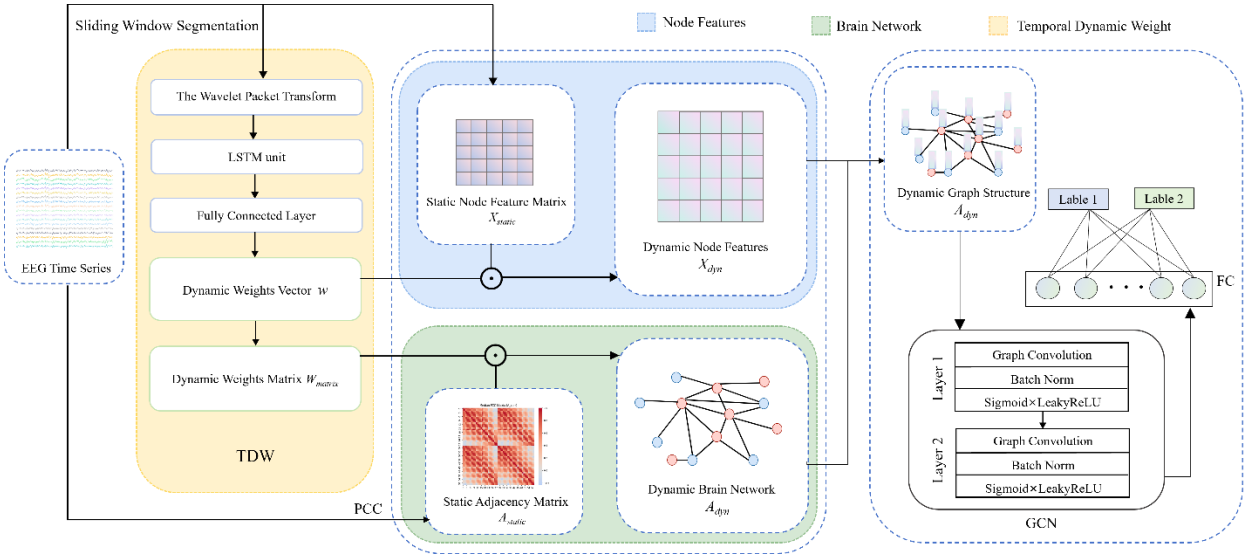

Figure 1. TDGCN model structure diagram

2.1. Temporal Dynamic Weight

In the construction of temporal dynamic weight, this paper employs a sliding window approach to extract wavelet packet statistical features for building the temporal input sequence. An LSTM is then utilized to generate dynamic connection weight associated with nodes across various brain regions. The TDW generation structure is shown in Figure 2, comprises four components: sliding window partitioning, WPT sub-band decomposition, sliding window feature sequence construction, and LSTM-based temporal dynamic weight generation. The specific process is described as follows.

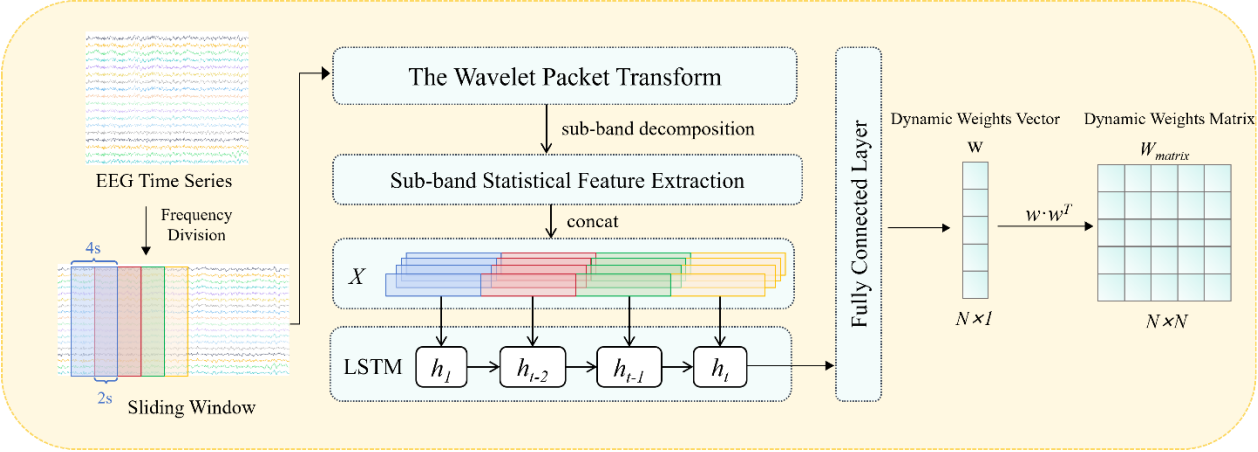

Figure 2. Temporal dynamic weight (TDW) Generation Structure

2.1.1. Sliding Window Partitioning

Divide each subject's 200-second EEG signal into five frequency bands. Then apply sliding window processing to each 10-second EEG sample using a 4-second window with a 2-second stride and 50% overlap. A 4-second window can cover typical EEG rhythm cycles, facilitating stable extraction of frequency-domain features [18]. Meanwhile, 50% overlap ensures temporal continuity while increasing sample size, enhancing the model's ability to perceive fine-grained changes [19, 20].

2.1.2. WPT Sub-band Decomposition

Each of the 59 channel signals within the sliding window undergoes a two-level wavelet packet decomposition using the Daubechies 4 wavelet basis function, yielding four sub-band components. WPT offers finer frequency resolution, enabling effective capture of the local spatiotemporal characteristics of EEG signals [21].

2.1.3. Sliding Window Feature Sequence

For each sub-band, extract four statistical features: mean, variance, energy, and entropy. Concatenate all channel features to form the feature vector $X_t \in R^{d_t}$ for the current window, where t =1, 2, 3, 4, $d_t = N \times N_b \times N_f$ (N =59 is the number of channels, N_b =4 is the number of sub-bands, and N_f =4 is the number of features). Each 10-second sample contains 4 windows, ultimately generating a feature sequence of length T=4: $X = [X_1, X_2, X_3, X_4] \in R^{T \times d_t}$, which serves as input for the subsequent LSTM model.

2.1.4. LSTM Temporal Dynamic Weight Generation

LSTM is suitable for modeling non-stationary EEG time series due to its robust ability to capture long-term dependencies [22]. By feeding sliding window feature sequences into the LSTM network, it outputs a sequence of hidden states at each time step:

$$f_t = \sigma(W_f [h_{t-1}, X_t] + b_f) \quad (1)$$

$$i_t = \sigma(W_i[h_{t-1}, X_t] + b_i) \tag{2}$$

$$C_t = \tanh(W_c[h_{t-1}, X_t] + b_c) \tag{3}$$

$$C_t = f_t * C_{t-1} + i_t * C_t \tag{4}$$

$$o_t = \sigma(W_o[h_{t-1}, X_t] + b_o) \tag{5}$$

$$h_t = o_t * \tanh(C_t) \tag{6}$$

Among these, f_t, i_t, o_t respectively denote the input gate, forget gate, and output gate; C_t represents the memory cell state; $W_f, W_i, W_c, W_o \in R^{d_h \times (d_t + d_h)}$ is the learnable parameter matrix; $b_f, b_i, b_c, b_o \in R^{d_h}$ is the bias vector; $\sigma(\cdot)$ denotes the Sigmoid activation function; X_t is the input at the current time step; h_{t-1} is the hidden state from the previous time step, $h_t \in R^{d_h}$ is the updated hidden state, assuming dimension $d_h = 64$.

Take the final hidden state h_t and map it through a fully connected layer to obtain the node dynamic weight vector $w \in R^N$.

$$w = \text{Sigmoid}(W_{fc} \cdot h_t + b) \tag{7}$$

$W_{fc} \in R^{N \times d_h}$ and $b \in R^N$ represent trainable parameters, where each element $w_i \in (0, 1)$ indicates the dynamic activity level of the i-th EEG channel within the current time slice. To construct the connection weight matrix between arbitrary node pairs, an unsqueeze operation is further applied to w, expanding its dimension to $w \in R^{N \times 1}$. A symmetric dynamic connection weight matrix is then constructed via the outer product:

$$W_{matrix} = w \cdot w^T \tag{8}$$

$W_{matrix} \in R^{N \times N}$ represents the degree of joint activity between any two brain regions and serves as a weight matrix that modulates static connection strengths during dynamic brain network construction.

2.2. Dual-Level Dynamic Brain Network Modeling.

To achieve dynamic modeling of brain functional connectivity networks, this paper introduces temporal dynamic mechanisms at both the node feature and graph structure levels.

2.2.1. Dynamic Node Feature

To enhance the discriminative power of node features, this study extracts DE and PSD features from 10-second EEG segments. By introducing the MCA for feature fusion, the complementary properties of DE and PSD in information complexity and energy distribution are leveraged [12], yielding a static node feature matrix.

Subsequently, utilizing the node dynamic weight vectors generated by LSTM, a residual weighting strategy is applied to dynamically weight static features, thereby generating a dynamic node feature matrix for graph convolutional input. The construction process is shown in Figure 3, with specific steps as follows.

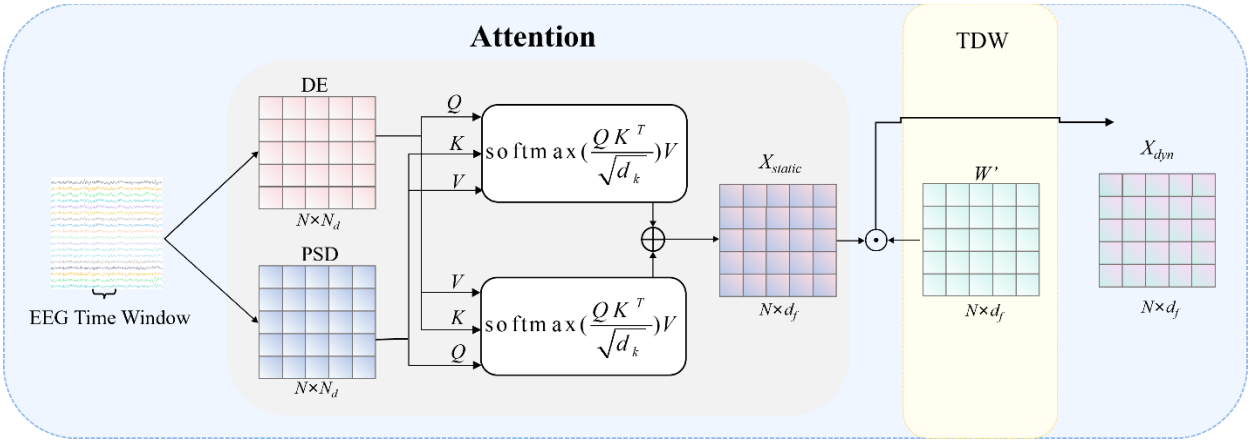

Figure 3. Process of constructing the dynamic node feature matrix

(1) DE Feature Extraction

DE is used to measure the information complexity of continuous variables. Its theoretical definition formula is as follows:

$$h(x) = -\int_{-\infty}^{\infty} p(x) \log p(x) dx \tag{9}$$

Where x is a general continuous random variable, and when the signal τ follows a Gaussian distribution $N(\mu, \sigma^2)$:

$$p(\tau) = \frac{1}{\sqrt{2\pi\sigma^2}} exp(-\frac{(\tau-\mu)^2}{2\sigma^2}) \tag{10}$$

Substituting into the defining expression yields the closed-form solution for the difference entropy $h(\tau)$ of the Gaussian-distributed random variable τ:

$$h(\tau) = \frac{1}{2} log(2\pi e\sigma^2) \tag{11}$$

Previous studies have demonstrated [23] that after bandpass filtering, EEG signals approximately follow a Gaussian distribution across a series of subbands, thereby satisfying the prerequisite for differential entropy calculation. Since multi-band feature combinations often yield superior classification performance compared to single-band inputs [24, 25], this study calculates variance σ^2 for each channel across five frequency bands to extract DE features, $F_{DE} \in R^{N \times N_d}$ serving as network input, where N_d =5 denotes the number of frequency bands.

(2) PSD Feature Extraction

PSD serves as a crucial metric for measuring signal energy distribution in frequency domain analysis. This paper employs the Welch method to compute the power spectral density of each channel signal [26], defaulting to Hanning windowing for weighted smoothing. This approach reduces spectral leakage and enhances the stability of spectral estimation [27]. The specific process is as follows.

Divide the original signal into K overlapping windows. Apply a window function to each segment and perform a Fast Fourier Transform (FFT) to compute the estimated power spectral density at frequency for the kth window segment:

$$p_k(f) = \frac{1}{W_L}\left|F_k(f)\right|^2 \tag{12}$$

Where f is the frequency variable $F_k(f)$ represent the spectral coefficient at frequency f for the kth window segment, and W_L denote the normalization factor of the window function with length L. Finally, averaging the spectral density values at frequency f across all window segments yields the power spectral density of the entire signal segment at that frequency:

$$P(f) = \frac{1}{K}\sum_{k=1}^{K} p_k(f) \tag{13}$$

To construct EEG node features, this paper performs discrete approximate integration of spectral density values across five frequency bands for each channel signal, obtaining the total power within each band to form a 5-dimensional PSD feature $F_{PSD} \in R^{N\times N_d}$ for each channel.

(3) Feature Fusion

This paper employs a bidirectional cross-attention mechanism [12] to fuse DE and PSD features. Calculations are performed using Scaled Dot-Product Attention [28]:

$$\text{Attention}(Q,K,V) = \text{softmax}(\frac{QK^T}{\sqrt{d_k}})V \tag{14}$$

Where d_k represents the size of the last dimension of the query vector. The original F_{DE} and F_{PSD} are mapped to the query matrix Q, key matrix K, and value matrix V in the attention mechanism via $Q = FW_Q$, $K = F'W_K$, and $V = F'W_V$, respectively. In this process, F and F' correspond to either F_{DE} or F_{PSD}, while $W_* \in R^{N_d\times d_f}$ denotes the learnable linear mapping weights. The output dimension is set to $d_f = 64$. Compute the attention outputs for each direction separately:

$$A_1 = \text{Attention}(F_{DE}, F_{PSD}, F_{PSD}) \tag{15}$$

$$A_2 = \text{Attention}(F_{PSD}, F_{DE}, F_{DE}) \tag{16}$$

Sum the results to obtain the fused node feature matrix $X_{static} \in R^{N\times d_f}$:

$$X_{static} = A_1 + A_2 \tag{17}$$

(4) Dynamic Node Feature Matrix

Based on the dynamic weight vector $w \in R^{N\times 1}$ output by the LSTM, the residual weighting method is applied to the static feature vector $x_i \in R^{d_f}$ of each node i. Its dynamic feature representation is:

$$x_i^{dyn} = x_i + w_i \cdot x_i = (1+w_i)\cdot x_i \tag{18}$$

Perform element-wise multiplication between $W' = 1+w$ and X_{static} to obtain the dynamic feature matrix:

$$X_{dyn} = X_{static} \odot (1 + w) \tag{19}$$

Where $\odot$ denotes the Hadamard product (element-wise multiplication). During multiplication, w is automatically broadcast to $w \in R^{N \times d_f}$, thereby enabling dynamic weighting of each node's features. $X_{dyn} \in R^{N \times d_f}$ provides more discriminative node inputs during feature propagation.

2.2.2. Dynamic graph structure

The Pearson correlation coefficient (PCC) between channels is computed from multi-frequency signals. A static functional connectivity graph is constructed as the base structure. A dynamic node weight matrix is introduced to dynamically adjust the edge weights, resulting in a time-varying adjacency matrix, i.e., the dynamic brain network. The construction process is shown in Figure 4. The specific steps are as follows.

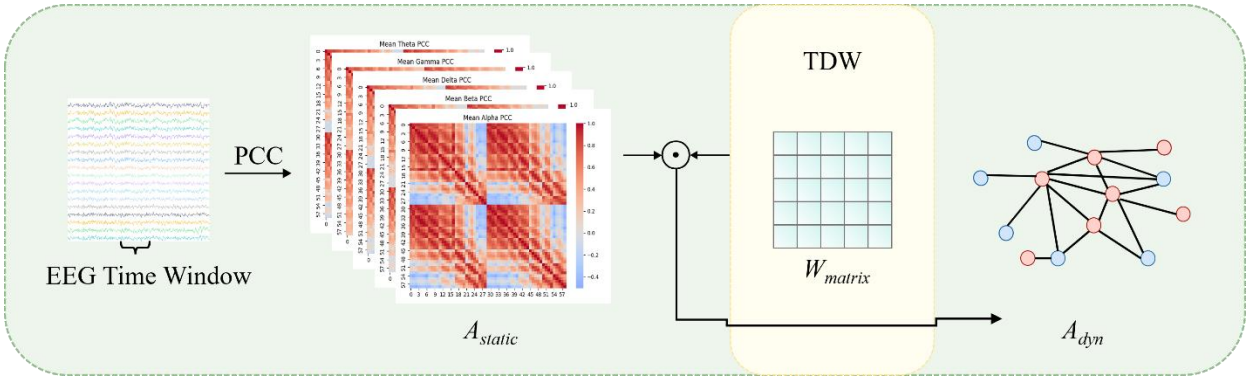

Figure 4. Structure for generating dynamic graphs

(1) Static Functional Connectivity Graph

Previous research by our team confirmed that the brain functional connectivity graph constructed based on the PCC demonstrates stable and robust performance in schizophrenia classification tasks [29]. In this study, we employed the PCC to compute the correlation between corresponding time series of any two EEG channels for signals across all frequency bands:

$$\mathrm{PCC}(X_i, X_j) = \frac{\mathrm{Cov}(X_i, X_j)}{\sigma_{X_i} \cdot \sigma_{X_j}} \tag{20}$$

Where X_i and X_j are the EEG time series for channels i and j, respectively, $\mathrm{Cov}(X_i, X_j)$ is the covariance, and σ_{X_i} and σ_{X_j} are the standard deviations. The basic correlation matrices for the five frequency bands are calculated to construct the initial adjacency matrix $A_{static} \in R^{N \times N}$.

(2) Dynamic Weighting Mechanism

Since the validity of edge connections depends not only on the statistical correlations between channels but also on the active status of the channels themselves, the dynamic weight matrix $W_{matrix} = w \cdot w^T \in R^{N \times N}$ output by the TDW module is introduced. This paper multiplies the static correlation matrix $A_{static} \in R^{N \times N}$ element-wise with W_{matrix} to generate the final dynamic adjacency matrix $A_{dyn} \in R^{N \times N}$:

$$A_{dyn} = A_{static} \odot W_{matrix} \tag{21}$$

Where the i-th and j-th elements of W_{matrix} are w_i, and w_j, respectively, then the weight of each connection in the dynamic adjacency matrix A is given by:

$$\left(A_{dyn}\right)_{i,j} = \left(A_{static}\right)_{i,j} \cdot w_i \cdot w_j \tag{22}$$

The aforementioned dynamic weighting mechanism can be understood as soft gating for connection strength: if channels i and j exhibit high correlation and both demonstrate strong activity within the current time slice, the connection is retained and strengthened. Conversely, if a node's current state is weak, its connection weight will be reduced even if statistical correlation exists. This mechanism enhances the graph structure's ability to represent temporal state changes.

2.3. GCN Classification Framework

After obtaining the dynamic node feature matrix X_{dyn} and the dynamic graph adjacency matrix A_{dyn}, a two-layer graph convolutional network is employed for classification based on these dynamic structures.

The basic propagation mechanism of GCN is as follows:

$$H^{(l+1)} = \sigma(\tilde{D}^{-\frac{1}{2}}\tilde{A}\tilde{D}^{-\frac{1}{2}}H^{(l)}W^{(l)}) \tag{23}$$

Where I denotes the identity matrix, $\tilde{A} = A_{dyn} + I$ denotes the adjacency matrix with self-loops added to the dynamic graph structure, $\tilde{D}$ is the corresponding degree matrix, $\tilde{D}_{ii} = \sum_j \tilde{A}_{ij}$, l denotes the number of convolutional layers, $H^{(l)} \in R^{N\times d}$ represents the node feature matrix of layer l, where d is the dimension of node features, $H^{(0)} = X_{dyn}$, W is the learnable parameter matrix of this layer, where F is the dimension of the output features, and $H^{(l+1)} \in R^{N\times F}$ is the output feature matrix.

To enhance the ability to identify key channels, this paper introduces a channel-wise gating mechanism [16] after the convolutional output of each layer. Following batch normalization, $\mathrm{split}(\cdot)$ divides the output features into two groups along the channel dimension: a gating branch $H_{gate} \in R^{N\times d/2}$ and a feature branch $H_{value} \in R^{N\times d/2}$. After computing the gating and feature responses, they are fused to obtain the input features for the next layer. The specific formula is as follows.

$$(H_{gate}, H_{value}) = \mathrm{split}(H^{(l+1)}) \tag{24}$$

$$H^{(l+1)} = \mathrm{Sigmoid}(H_{gate}) \odot \mathrm{LeakyReLU}(H_{value}) \tag{25}$$

The second layer adopts the same structure as the first layer, employing the GCN-BN-Gate architecture. The gated output features from the first layer serve as the input for the second layer. The output undergoes global average pooling before being fed into a fully connected layer and a $\mathrm{Softmax}$ classifier to complete the classification task.

Each of the two graph convolutional layers has 64 output channels, which are compressed to 32 dimensions via a channel gating mechanism after convolution. Following the second graph

convolutional layer, global average pooling is applied, and the classification result is output through a fully connected layer reducing dimensions from 32 to 2.

3. EXPERIMENTAL SETTING AND RESULTS ANALYSIS

3.1. Dataset

The data used in this study were obtained from Beijing Huilongguan Hospital, comprising 59-channel EEG recordings collected from 103 first-episode schizophrenia patients and 92 matched healthy controls during closed-eye resting state [10]. Participants were matched for gender, age, and education level. Demographic characteristics and clinical data, including PANSS scores, for both groups are summarized in Table 1.

Table 1. Demographic and clinical data of the two groups of subjects

Features	Schizophrenic (n = 103)	Healthy subjects (n = 92)	Statistical values
Average age (years)	30.55±8.002	30.55±7.287	F1,195< 1
Length of schooling (years)	14.17±2.494	14.79±2.557	F1,195= 3.022, p = 0.084
Sex (male/female)	51/52	48/44	c12= 0.182, p = 0.670
PANSS scores	74.31±10.87		
Positive score	20.53±4.72		
Negative scores	17.18±5.63		

Raw EEG data were preprocessed using EEGLAB [30], with electrodes positioned using the default BESA electrode template. The reference electrode was converted to an average reference. The EEG signals were then bandpass-filtered between 1 and 50 Hz, with a 50 Hz notch filter applied. Independent Component Analysis (ICA) was applied to remove eye and muscle activity artifacts. Bad leads were interpolated, and corrupted segments were removed. The EEG data underwent resampling and frequency division processing, standardizing the sampling rate to 500 Hz and filtering the signals into five frequency bands: Delta (1-3 Hz), Theta (4-7Hz), Alpha (8-12Hz), Beta (13-30Hz), and Gamma (31-49Hz). After removing redundant electrodes, 59 electrode channels were selected as EEG nodes to provide the foundation for subsequent feature extraction.

3.2. Experimental Setting

The experiment used 10-fold cross-validation, randomly dividing the dataset into 10 folds. In each iteration, one fold was selected as the test set, with the remaining nine folds used for training. The final model performance was evaluated by averaging the results from all 10 iterations. Training was performed using the Adam optimizer with an initial learning rate of 0.001, weight decay of 1e-4, and cross-entropy loss as the objective function. Additionally, a learning rate scheduling strategy and an early stopping mechanism were implemented. When the validation set accuracy failed to improve for five consecutive epochs, the learning rate was halved. If no improvement occurred for ten consecutive epochs, training was terminated early to prevent overfitting. The maximum training epochs were set to 200, with a batch size of 64.

3.3. Results

This paper independently trained models on five classic frequency bands: Delta, Theta, Alpha, Beta, and Gamma, and compared their classification performance. The results are shown in Table 2. Where these are, the Gamma band demonstrated the most outstanding performance, achieving an accuracy rate of 93.85% and an AUC of 94.16%; it also attained the best values across all other metrics.

Additionally, the model demonstrated superior performance in the Beta band, significantly outperforming lower frequency bands such as Theta and Alpha. This further suggests that mid-to-high frequency EEG activity may carry more pathological information associated with schizophrenia.

Table 2. Experimental results across different EEG frequency bands

Frequency band	Accuracy (%)	Precision (%)	Recall (%)	F1-score (%)	AUC (%)
Alpha	79.74	82.78	75.63	79.05	79.79
Beta	87.18	85.44	89.80	87.56	87.17
Delta	82.56	84.06	83.25	83.65	82.51
Gamma	93.85	94.82	92.89	93.72	94.16
Theta	79.23	82.65	78.28	80.00	79.36

The experimental results above indicate that functional connectivity changes under the Gamma rhythm are most pronounced in schizophrenia classification tasks, validating the effectiveness of the temporal dynamic modeling mechanism proposed in this paper. By capturing the dynamic evolution of node and connection relationships within this frequency band, the TDGCN model achieves high-precision recognition of schizophrenia brain states, demonstrating the advantages of dynamic graph neural networks in modeling spatiotemporal EEG features.

3.4. Ablation experiments

To further evaluate the independent contributions of key modules within the TDGCN model, this paper designed four ablation structures and conducted comparative experiments in the gamma band. TDGCN-noW: Removes the temporal dynamic weights generated by LSTM, using only static node features and static graph structure; TDGCN-noF: Removes dynamic node features, retaining only static node features and dynamic graph structure; TDGCN-noS: Removes dynamic graph structure, retaining only dynamic node features and static graph structure; TDGCN-noGate: Removes only the channel attention gating mechanism. Table 3 presents a comparison of the classification performance of each model in the Gamma band.

Table 3. Ablation experiment results for different modules of TDGCN

Methodology	Accuracy (%)	Precision (%)	Recall (%)	F1-score (%)	AUC (%)
TDGCN-noW	81.74	83.01	80.36	81.63	81.45
TDGCN-noF	88.92	89.85	87.63	88.72	88.91
TDGCN-noS	87.56	88.73	86.28	87.49	87.63
TDGCN-noGate	92.41	93.02	91.34	92.17	92.21
TDGCN	93.85	94.82	92.89	93.72	94.16

The results indicate that the complete TDGCN model achieves optimal performance across all evaluation metrics, where temporal dynamic weights contribute most significantly to model performance. Removing this module caused the model accuracy to drop from 93.85% to 81.72% and the AUC to decrease from 94.16% to 81.45%, confirming the critical role of temporal dynamic weights in capturing the complex spatiotemporal dependencies of EEG's non-stationary characteristics during modeling.

Additionally, removing either the dynamic node features (TDGCN-noF) or the dynamic graph structure (TDGCN-noS) resulted in a performance drop of approximately 5%–6%, indicating a significant synergistic effect between the two submodules. Together, they jointly construct a high-quality graph structure representation and spatio-temporal modeling capability. While removing the gating mechanism (TDGCN-noGate) had a relatively minor impact on the model's overall performance, it still played a positive role in model convergence and feature regulation.

In summary, the ablation experiments validate that the performance advantages of TDGCN stem from the synergistic interaction of multiple modules—including temporal modeling, dynamic graph structure, and channel regulation—rather than improvements in any single component. This fully demonstrates its effectiveness and sound design in modeling EEG spatiotemporal features.

3.5. Comparison experiment

To objectively evaluate the performance of the TDGCN model, this paper selected SVM, EEGNet, and LSTM as baseline models. Gamma band data was chosen, and identical training-testing splits and feature inputs were constructed under the same preprocessing workflow and evaluation metrics for comparison with the proposed model. The results are shown in Table 4.

Table 4. Results of comparison experiment

Methodology	Accuracy (%)	Precision (%)	Recall (%)	F1-score (%)	AUC (%)
SVM	78.21	77.29	79.90	79.71	85.45
EEGNET	85.90	86.34	85.35	86.28	86.19
LSTM	87.95	88.68	89.10	88.89	89.95
TDGCN	93.85	94.82	92.89	93.72	94.16

Experimental results demonstrate that TDGCN outperforms the baseline model across all metrics, where the F1-score reaches 93.72% and the AUC reaches 94.16%. Analysis indicates that while LSTM can model temporal information, it neglects spatial topological relationships between channels; EEGNet possesses some spatial feature extraction capabilities but cannot explicitly construct and utilize global functional connections between channels like graph neural networks. As a traditional classifier, SVM exhibits limited expressive power when handling high-dimensional nonlinear EEG data. In contrast, TDGCN effectively integrates spatiotemporal information through dual-level dynamic modeling of node features and graph structure, enabling efficient identification of brain network features in schizophrenia. This demonstrates its significant advantages in modeling complex brain states.

4. CONCLUSION

This paper proposes the TDGCN model for schizophrenia identification, introducing dynamic modeling mechanisms at both node feature and graph structure levels to achieve efficient spatiotemporal joint modeling of EEG signals. Experimental results demonstrate that TDGCN outperforms competing methods across multiple evaluation metrics, validating the critical role of temporal modeling and dynamic graph structures in enhancing model performance. This study offers novel insights for EEG analysis based on dynamic graph networks and confirms the method's potential in supporting psychiatric diagnosis. Future work will focus on adaptive parameter optimization, multimodal data fusion, and cross-center validation to further enhance its clinical applicability.

REFERENCES

[1] Saha S, Chant D, Welham J, et al. A systematic review of the prevalence of schizophrenia. PLoS medicine, 2005, 2(5): e141. PLoS medicine. 2005, Vol. 2 (No. 5), p. e141.

[2] McDonald J, Lee E, Ibrahim S, et al. Prevalence of subjective and objective sleep disturbances: comparing persons with Schizophrenia and non-psychiatric comparisons. The American Journal of Geriatric Psychiatry. 2024, Vol. 32 (No. 4), p. S123-S124.

[3] Sarisik E, Popovic D, Keeser D, et al. EEG-based signatures of schizophrenia, depression, and aberrant aging: a supervised machine learning investigation. Schizophrenia Bulletin. 2025, Vol. 51 (No. 3), p. 804-817.

[4] Jafari M, Shoeibi A, Khodatars M, et al. Emotion recognition in EEG signals using deep learning methods: A review. Computers in Biology and Medicine. 2023, Vol. 165, p. 107450.

[5] Senthil Kumar S, Venmathi A R, Thangavel Y, et al. ResDense Fusion: enhancing schizophrenia disorder detection in EEG data through ensemble fusion of deep learning models. Neural Computing and Applications. 2025, Vol. 37 (No. 4), p. 2411-2433.

[6] Cheng C, Liu W, Jia Z, et al. A Multi-stage Hemisphere Asymmetry Fusion Network Inspired by the brain for EEG depression detection. Information Fusion. 2025, Vol. 124, p. 103342

[7] Li Y, Li K, Wang S, et al. A spatiotemporal separable graph convolutional network for oddball paradigm classification under different cognitive-load scenarios. Expert Systems with Applications. 2025, Vol. 262, p. 125303.

[8] Graña M, Morais-Quilez I. A review of Graph Neural Networks for Electroencephalography data analysis. Neurocomputing. 2023, Vol. 562, p. 126901.

[9] Tang H, Xie S, Xie X, et al. Multi-domain based dynamic graph representation learning for EEG emotion recognition. IEEE Journal of Biomedical and Health Informatics. 2024, Vol. 28(No. 9), p. 5227-5238.

[10] Yin G, Chang Y, Zhao Y, et al. Automatic recognition of schizophrenia from brain-network features using graph convolutional neural network. Asian Journal of Psychiatry. 2023, Vol. 87, p. 103687.

[11] Zhong W, Zhang Y, Fu P, et al. A spatio-temporal graph convolutional network for gesture recognition from high-density electromyography. 2023 29th International Conference on Mechatronics and Machine Vision in Practice (M2VIP). Queenstown, New Zealand, 2023, p. 1-6.

[12] Zhao Y, Gu J. Feature fusion based on Mutual-Cross-Attention mechanism for EEG emotion recognition. International Conference on Medical Image Computing and Computer-Assisted Intervention (MICCAI 2024). Marrakesh, Morocco, 2024, p. 276-285.

[13] Guo J, Chen C L P, Liu Z, et al. Dynamic neural network structure: A review for its theories and applications. IEEE Transactions on Neural Networks and Learning Systems. 2024, Vol. 36 (No. 3), p. 4246-4266.

[14] Liang G, Tiwari P, Nowaczyk S, et al. Dynamic causal explanation based diffusion - variational diffusion-variational graph neural network for spatiotemporal forecasting. IEEE Transactions on Neural Networks and Learning Systems. 2024, Vol. 36(No. 5), p. 9524-9537.

[15] Xiao M, Zhu Z, Xie K, et al. MEEG and AT-DGNN: Improving EEG Emotion Recognition with Music Introducing and Graph-based Learning. 2024 IEEE International Conference on Bioinformatics and Biomedicine (BIBM). Lisbon, Portugal, 2024, p. 4201-4208.

[16] Guo K, Hu Y, Qian Z, et al. Dynamic graph convolution network for traffic forecasting based on latent network of Laplace matrix estimation. IEEE Transactions on Intelligent Transportation Systems. 2020, Vol. 23 (No. 2), p. 1009-1018.

[17] Leng Y, Cui W, Bai C, et al. Dynamic structural brain network construction by hierarchical prototype embedding GCN using T1-MR. International conference on medical image computing and computer-assisted intervention(MICCAI 2023). Vancouver, BC, Canada, 2023, p. 120-130.

[18] Góngora L, Paglialonga A, Mastropietro A, et al. A novel approach for segment-length selection based on stationarity to perform effective connectivity analysis applied to resting-state eeg signals. Sensors. 2022, Vol. 22 (No. 13), p. 4747.

[19] Alkahtani H, Aldhyani T H H, Ahmed Z A T, et al. Developing system-based artificial intelligence models for detecting the attention deficit hyperactivity disorder. Mathematics. 2023, Vol. 11 (No. 22), p. 4698.

[20] Ingolfsson T M, Benatti S, Wang X, et al. Minimizing artifact-induced false-alarms for seizure detection in wearable EEG devices with gradient-boosted tree classifiers. Scientific reports. 2024, Vol. 14 (No. 1), p. 2980.

[21] Frusque G, Fink O. Robust time series denoising with learnable wavelet packet transform. Advanced Engineering Informatics. 2024, Vol. 62, p. 102669.

[22] Perumal T, Mustapha N, Mohamed R, et al. A comprehensive overview and comparative analysis on deep learning models. Journal Of Artificial Intelligence Research. 2024, Vol. 6 (No. 1), p. 301-360.

[23] Shi L C, Jiao Y Y, Lu B L. Differential entropy feature for EEG-based vigilance estimation. 2013 35th Annual International Conference of the IEEE Engineering in Medicine and Biology Society (EMBC). Osaka, Japan, 2013, p. 6627-6630.

[24] Zhang Z, Meng Q, Jin L C, et al. A novel EEG-based graph convolution network for depression detection: incorporating secondary subject partitioning and attention mechanism. Expert Systems with Applications. 2024, Vol. 239, p. 122356.

[25] Jiang C, Li Y, Tang Y, et al. Enhancing EEG-based classification of depression patients using spatial information. IEEE transactions on neural systems and rehabilitation engineering. 2021, Vol. 29, p. 566-575.

[26] Simfukwe C, Youn Y C, An S S. qEEG as Biomarker for Alzheimer's Disease: Investigating Relative PSD Difference and Coherence Analysis. Alzheimer's & Dementia. 2024, Vol. 20, p. e088587.

[27] Siva A S, Rameshkumar S G, Dhayalini K. Supraharmonic Analysis by Welch's-Power Spectral Density Estimation. 2024 Third International Conference on Power, Control and Computing Technologies (ICPC2T). Raipur, India, 2024, p. 357-362.

[28] Groot D J, Ellerbroek J, Hoekstra J M. Comparing attention-based methods with long short-term memory for state encoding in reinforcement learning-based separation management. Engineering Applications of Artificial Intelligence. 2025, Vol. 159, p. 111592.

[29] Yin G, Yuan J, Chen Y, et al. Schizophrenia recognition based on three-dimensional adaptive graph convolutional neural network. Scientific Reports. 2025, Vol. 15 (No. 1), p. 4067.

[30] Delorme A, Makeig S. EEGLAB: an open source toolbox for analysis of single-trial EEG dynamics including independent component analysis. Journal of neuroscience methods. 2004, Vol. 134 (No. 1), p. 9-21.